LBL-27742
UC 600

# Lawrence Berkeley Laboratory
UNIVERSITY OF CALIFORNIA

## APPLIED SCIENCE DIVISION

Presented at the Indoor Air '90 Conference,
Toronto, Canada, July 29–August 3, 1990,
and to be published in the Proceedings

**Modeling Radon Entry into Houses with Basements: Model Description and Verification**

K.L. Revzan, W.J. Fisk, and A.J. Gadgil

January 1991



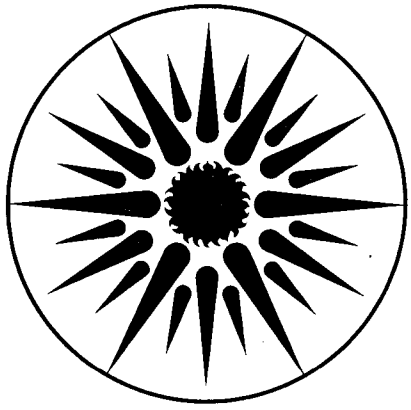

APPLIED SCIENCE
DIVISION



Prepared for the U.S. Department of Energy under Contract Number DE-AC03-76SF00098.

To be published in
*Indoor Air*

LBL-27742

# MODELING RADON ENTRY INTO HOUSES WITH BASEMENTS: MODEL DESCRIPTION AND VERIFICATION

K.L. Revzan, W.J. Fisk, A.J. Gadgil
Indoor Environment Program
Applied Science Division
Lawrence Berkeley Laboratory
1 Cyclotron Road
Berkeley, CA 94720

January, 1991

This work was supported by the Director, Office of Energy Research, Office of Health and Environmental Research, Ecological Research Division, Human Health and Assessments Division, and Pollutant Characterization and Safety Research Division and by the Assistant Secretary for Conservation and Renewable Energy, Office of Building and Community Systems, Building Systems Division of the U.S. Department of Energy (DOE) under Contract No. DE-AC03-76SF00098.

## Abstract

We model radon entry into basements using a previously developed three-dimensional steady-state finite difference model that has been modified in the following ways: first, cylindrical coordinates are used to take advantage of the symmetry of the problem in the horizontal plane, thereby increasing resolution and computing efficiency without significant loss of generality; second, the configuration of the basement has been made more realistic by incorporating the concrete footer which supports the basement walls and floor; third, a quadratic relationship between the pressure and flow in the L-shaped gap between slab, footer, and wall has been employed; fourth, the natural convection of the soil gas which follows from the heating of the basement in winter has been taken into account. The temperature field in the soil is determined from the equation of energy conservation, using the basement, surface, and deep-soil temperatures as boundary conditions. The pressure field is determined from Darcy's law and the equation of mass conservation (continuity), assuming that there is no flow across any boundary except the soil surface (atmospheric pressure) and the opening in the basement shell (fixed pressure). Since the energy conservation equation includes both heat advection and conduction, the temperature and pressure equations must be coupled. After the pressure and temperature fields have been obtained, the velocity field is found from Darcy's law. Finally, the radon concentration field is found from the equation of mass-transport, assuming that diffusive entry through openings may be neglected. The convective radon entry rate through the opening or openings is then calculated. In this paper we describe the modified model, compare the predicted radon entry rates with and without the consideration of thermal convection, and compare the predicted rates with rates determined from data from 7 houses in the Spokane River valley of Washington and Idaho. Although the predicted rate is much lower than the mean of the rates determined from measurements, errors in the measurement of soil permeability and variations in the permeability of the area immediately under the basement slab, which has a significant influence on the pressure field, can account for the range of entry rates inferred from the data.

Keywords: Radon, Modeling, Soil, Mass transport, Pollutant, Heat transfer

## Introduction

The primary source of radon in houses with high indoor concentrations is, in most cases, the surrounding soil; the primary means of entry is generally the passage of soil-gas through cracks or other gaps in the building shell (Nero, 1988a) or through permeable sub-surface walls (Garbesi and Sextro, 1990). In houses with basements, for which the length of the soil-gas path from soil surface to entry point may be long and the pore-space radon concentration consequently elevated, radon entry rates may be particularly high. The soil-gas flow rate is primarily dependent on the permeability of the soil, on the nature of openings in the building shell, and on the degree of basement depressurization. The radon concentration in the soil is dependent on the soil gas velocity, the radium content, porosity, density, and emanating fraction of the soil, the diffusivity of radon in the soil, and the depth.

A model amenable to closed-form solutions can provide only a crude representation of the problem. One such model is described by Mowris and Fisk (1987) and by Nazaroff (1988b). A linear crack in the basement slab is represented in bipolar coordinates by a cylinder embedded in a homogeneous semi-infinite medium; the soil surface is represented by a plane parallel to the axis of the cylinder. The basement itself is not modeled. Darcy's law and the continuity equation, which together describe soil-gas transport, reduce to the Laplace equation for the pressure field; this equation has a series solution. The mass-transport equation without diffusion may then be solved for the radon concentration field, assuming a fixed concentration at infinite radius, and the two solutions combined to give the radon entry rate at the cylinder. This model gives an indication of the dependence of the entry rate on basement pressure and soil permeability when the soil is homogeneous, but it cannot represent the basement-soil boundary correctly, nor can it deal with inhomogeneous soils.

Recognition of the limitations of closed-form models has led to the development of numerical models, such as the two-dimensional models of Dimbylow (1987) and of Mowris and Fisk (1987), and the three-dimensional model of Loureiro (1987) and Loureiro, *et al.* (1990), which are able to deal with irregular boundaries and arbitrary boundary conditions. Here, steady-state solutions of the generalized Laplace equation and the mass-transport equation are given in Cartesian coordinates for a region comprising a quadrant of a basement and a block of soil large enough that a further increase in size produces an insignificant change in the soil-gas and radon entry rates. The basement walls and slab and the outer limits of the soil block are treated as no-flow boundaries, while the soil surface is a boundary at atmospheric pressure and zero radon concentration. In the Loureiro model, the pressure, soil-gas velocity, and radon concentration in peripheral gaps (of rectangular cross-section) in the basement slab are modeled analytically and the results adjusted to match those of the numerical solution at the soil-gap interface. The variability of the soil characteristics is essentially unlimited, although variation on a fine scale may lead to an excessively large number of control volumes, long solution times, and large computing costs.

In this paper, we describe a steady-state numerical model based on that of Loureiro, but one that takes advantage of the symmetry of the problem in the horizontal plane by using cylindrical coordinates. There is a loss of generality in that only central and peripheral openings in the basement shell can be modeled, but these are, in fact, the only types considered in earlier work. The

model has also been modified so that the concrete footer that normally supports the wall and slab is be included, giving the slab-footer-wall gap an L-shape. The boundary conditions at the soil-gap interface have been altered in order to take this shape into consideration. This gap, which is considered to be an important source of indoor radon in many houses, is the only opening in the building shell discussed in detail in this paper; for a description of models with alternative or additional openings, see Revzan and Fisk (1990b) and Garbesi and Sextro (1990). The Loureiro model neglects the circulation of soil gas which occurs in winter and is caused by the presence of a heated basement; we incorporate this circulation into the model and demonstrate that buoyancy forces acting on soil gas may be an important factor in radon entry. Finally, to verify the numerical model to the limited extent possible, we compare the predictions of the model for the soil of the Spokane River Valley of Washington and Idaho with data from seven houses in that area. The influence of soil characteristics on radon entry is discussed in detail in Revzan (1990a).

## Model Description

The region to be modeled comprises the subsurface part of a basement and a block of the surrounding soil. Air is assumed to enter the basement solely through an L-shaped gap between the foundation footer, the slab, and the walls. (Gaps and cracks at other locations are discussed in Revzan and Fisk, 1990b.) Assuming that the cross-section of the walls and gaps does not vary, the basement can be modeled as a cylinder with only the loss of corner effects, which will be shown to be unimportant. The region from which a house draws soil gas depends on the positions of adjacent houses, the extent of their depressurization, and the characteristics of the soil. The exact boundaries of this region are likely to be important in particular cases, but in the general case, the soil block may be represented as well by a cylinder as by a box. The entire region may therefore be modeled in cylindrical coordinates, which permits greater resolution, shorter solution time (with lower cost), or a combination of the two. A vertical cross-section of the region, with the dimensions used in this paper, is shown in Figure 1. A detail of the cross-section of the basement area, with the width of the gap greatly exaggerated, is shown in Figure 2. In this paper, the gap width, w, is assumed to be 0.003 m and the thickness, t, to be 0.25 m.

The model comprises three differential equations. First, the temperature field in the soil is found from the steady-state energy conservation equation (assuming thermal equilibrium between the solid and gaseous phases of the soil [Bejan, 1984; Ene and Polisevski, 1987]),

$$\frac{1}{\rho_0}\nabla\cdot\left[\rho(r,z)\vec{v}(r,z)T(r,z)\right] = \nabla\cdot\left[\alpha(r,z)\nabla T(r,z)\right], \qquad (1)$$

where $\rho_0$ is the density of air at 0° C, T is the temperature, $\alpha$ is the thermal diffusivity at 0° C, and $\vec{v}$ is the soil-gas velocity. We assume that $\alpha = 5\times10^{-7}$ m$^2$ s$^{-1}$ throughout the soil (Oke, 1987). The temperature is fixed at $T_b$ at the outside of the basement, including the soil-gap interface, at $T_o$ at the soil surface ("outside", z=0), and at $T_s$ at the lower limit of the soil (z=12.1 m, Figure 1). The outer limit of the soil (r=15.15 m, Figure 1) is presumed to represent the boundary between two houses, so that here there is no heat flow, *i.e.*, the normal derivative of T must vanish. These boundary conditions are shown in Figures 1 and 2. Since the soil-gas velocity is

determined by the pressure and temperature fields, the heat-transfer and pressure equations must be coupled. In many cases of practical importance, however, heat advection is negligible with respect to conduction, so that the left-hand side of Equation 1 may be set to zero and the temperature field determined independently of the pressure field. The circumstances under which heat advection is significant will be described in the following section.

Next, the pressure field is found from a generalization of Darcy's law, *i.e.*,

$$\vec{v}(r,z) = -\frac{k(r,z)}{\mu}\left[\nabla P(r,z) - \rho(r,z) g\hat{z}\right], \tag{2}$$

where k the permeability of the soil, which is assumed to be isotropic, $\mu$ the viscosity of air ($1.8 \times 10^{-5}$ kg m$^{-1}$ s$^{-1}$), P the absolute pressure, $\rho$ the density of air, g the acceleration of gravity, and $\hat{z}$ the unit vector in the z-direction, taken positive downward. For temperatures of interest here, the dependence of $\rho$ upon T is given by

$$\rho(r,z) = \rho_0\left[1 - \beta T(r,z)\right], \tag{3}$$

where T is in °C, $\rho_0$ is the density of air at 0 °C (1.293 kg m$^{-3}$), and $\beta$ is the coefficient of thermal expansion, which is approximately equal to 1/273 °C$^{-1}$. For isothermal problems, it is customary to define a disturbance pressure by subtracting the atmospheric and static pressures from P. In our case, since the density of air varies with z, it is convenient to choose a reference density, which is arbitrary, rather than to use the integral expression for the static pressure. Boundary conditions are somewhat simplified if the reference is either $\rho_b$, the density where $T = T_b$, or $\rho_s$, the density where $T = T_s$. We choose the latter density and define the disturbance pressure, p, by the equation

$$p(r,z) = P(r,z) - P_A - \rho_s g z, \tag{4}$$

where $P_A$ is the atmospheric pressure, assumed constant in a steady-state model. Combining Equations 2, 3, and 4 gives

$$\vec{v}(r,z) = \frac{k(r,z)}{\mu}\left[\rho_0 g \beta[T_s - T(r,z)]\hat{z} - \nabla p(r,z)\right]. \tag{5}$$

The first term on the r.h.s. of this equation vanishes at the lower boundary of the soil, *i.e.*, when $T(r,z_s) = T_s$, so that the boundary condition here becomes simply a zero normal derivative. This convenience is the justification for the choice of $\rho_s$ as the reference density.

The equation of conservation of mass (continuity) is

$$\nabla \cdot \left[\rho(r,z)\vec{v}(r,z)\right] = 0. \tag{6}$$

Combining Equations 5 and 6, we have the second equation of the model, *i.e.*,

$$\nabla \cdot \left\{ \frac{\rho(r,z)k(r,z)}{\mu} \left[ \nabla p(r,z) + \rho_0 g \beta \left[ T(r,z) - T_s \right] \hat{z} \right] \right\} = 0. \tag{7}$$

This equation must be solved in conjunction with Equation 1 when thermal convection is significant.

The boundaries for the solution of equation 7 are the outer limit of the soil block in the r-direction, the soil surface and the lower limit of the soil block in the z-direction, and either the inner or outer basement surfaces, including the opening. If the inner basement surface is chosen as a boundary, the entire gap between slab and footer and wall and footer must be included in the problem. The gap width is typically four orders of magnitude smaller than the soil block size and the soil gas must change direction as it passes through the gap, so that the control volumes must be made very small in this region. As a result, computation time is high. In actual construction, moreover, the gap has irregular walls, so that it is not well represented by the model. Consequently, it is best to take the boundaries of the problem to be the outside surfaces of the basement and footer, including the mouth (soil-gap interface) of the slab-footer gap, and to treat the question of the gap itself separately. With these boundaries, radon entry by diffusion through concrete is neglected; this subject has been treated by Zapalac (1983). The question of radon entry through permeable walls is also neglected here, although the model is capable of treating the subject with only slight modifications. Garbesi and Sextro (1990) discuss soil-gas entry through permeable walls, but do not deal with radon entry *per se*.

Given these assumptions, the normal velocity must vanish at all concrete surfaces and at the outer and lower limits of the soil and the pressure must be fixed at the soil surface and the soil-gap interface. At vertical concrete surfaces and at the outer soil boundary, the vanishing of the normal velocity is equivalent to a zero normal pressure derivative. At horizontal concrete surfaces and at the lower soil boundary, Equation 5 gives

$$\frac{\partial p(r,z_s)}{\partial z} - \rho_0 \beta g \left[ T_s - T(r,z_s) \right] = 0, \tag{8}$$

where $z_s$ is the position of the surface of interest. At the lower soil boundary, this equation reduces to a vanishing normal derivative of p. At the soil surface, $z = 0$, $P = P_A$ and Equation 4 gives the boundary condition $p(r,0) = 0$. The boundary conditions at the three soil boundaries are shown on Figure 1.

The pressure at the soil-gap interface is determined by the basement pressure and the pressure drop across the gap. In winter, temperature differences between a house and the outside, the effect of wind, and the operation of heating, ventilation, and air-conditioning systems produce a basement pressure which is generally lower than $P_A$ (Feustel and Sherman, 1989; Sherman, *et al.*, 1979; Revzan, *et al.*, 1988; Revzan, 1989). The difference between the pressure at the basement side of the slab-wall gap and $P_A$, corrected for the static pressure difference, is written as $\Delta P_b$. The pressure drop across the gap, $\Delta P_g$, is determined from an algorithm due to Baker, *et al.*, (1989):

$$|\Delta P_g| = \frac{12\mu t}{w^2}|\vec{v}| + \frac{\rho(1.5+n)}{2}v^2. \tag{9}$$

Here, t and w are, respectively, the thickness and width of the opening (see Figure 2), v is the average speed of air through the opening, *i.e.*, the flow rate through the opening divided by the area, and n is the number of bends in the opening. Assuming that the temperature is constant inside the gap, so that there is no thermally-induced pressure difference between the basement and soil sides, the disturbance pressure at the soil-gap interface is then

$$p(r_g, z) = \Delta P_b + |\Delta P_g| + \rho_o \beta g (T_s - T_b) z, \tag{10}$$

where $r_g$ is the radial coordinate of the soil side of the gap. The boundary conditions at the basement may be clarified by examining Figure 2.

Having found a solution to Equation 7, we may determine the soil-gas velocity from Equation 5. The soil-gas entry rate, $E_s$, is then given by

$$E_s = \int_{\Sigma} \vec{v}(r_g, z) \cdot d\vec{\sigma}(r_g, z), \tag{11}$$

where $\vec{\sigma}$ is an element of the area of the soil-gap interface and $\Sigma$ indicates an integral over the entire interface area.

Finally, the radon concentration in the soil gas, C, is determined from

$$\nabla \cdot \left[\vec{v}(r,z) C(r,z)\right] = \nabla \cdot \left[D(r,z) \nabla C(r,z)\right] - \varepsilon(r,z) \lambda C(r,z) + \varepsilon(r,z) S(r,z), \tag{12}$$

where D is the bulk diffusivity of radon in soil, $\lambda$ the radon decay constant, $\varepsilon$ the porosity of the soil, and S the rate of release of radon into the soil gas per unit volume of soil. In this paper, we assume that the soil is homogeneous with $D = 10^{-6}\ m^2\ s^{-1}$ and $\varepsilon = 0.5$ (Nazaroff, 1988a). The model does not deal with spatial variations in soil moisture; values of D, $\varepsilon$, and S may be chosen to reflect wet conditions. The boundary conditions for solution of Equation 12 are identical to those for Equation 7 except at the soil-gap interface. At the soil surface, we assume C = 0; because radon concentrations in soil gas are typically high compared to those in the atmosphere, the assumption of a non-zero soil-surface concentration has a negligible effect on the result. We assume that radon entry by diffusion through a gap is negligible compared to convective entry. In that case, the radon concentration immediately inside the gap is equal to that immediately outside, *i.e.*, the normal derivative of C vanishes at the soil-gap interface. Other assumptions may be made, *e.g.*, that the concentration inside an opening has an exponential profile, but the effect on the calculated radon entry rate is negligible in situations where the rate is high enough to produce elevated indoor concentrations (Loureiro, 1987; Loureiro, *et al.*, 1990).

The radon concentration at distances far from the soil surface and the basement, $C_\infty$, is given by

$$C_\infty = \frac{S}{\lambda}. \tag{13}$$

Since this paper does not deal with the soil characteristics that determine the radon source strength, we normalize C by $C_\infty$, so that results are independent of S. From previously-determined velocities and a solution to Equation 12, we find the normalized radon entry rate, $E_r$, from the equation

$$E_r = \frac{1}{C_\infty}\int_\Sigma C(r,z)\vec{v}(r,z)\cdot d\vec{\sigma}(r,z). \tag{14}$$

$E_r$ has the dimensions of a volumetric flow rate, but must be distinguished from the soil-gas entry rate. Because the concentration at any opening is less than $C_\infty$, $E_r$ is always less than $E_s$.

The equations for the temperature, pressure, and concentration fields (1, 7, and 12) are solved in sequence, each in the same way. An irregular grid, similar to that of Loureiro (1987) divides the region into control volumes, which may vary greatly in size, and the equation of interest is integrated over each of the volumes using a first-order central difference scheme. The result is a set of difference equations of the form

$$c_{nm}\psi_{nm} = l_{nm}\psi_{n-1\,m} + r_{nm}\psi_{n+1\,m} + t_{nm}\psi_{nm-1} + b_{nm}\psi_{nm+1} + s_{nm}, \tag{15}$$

where $\psi_{nm}$ represents the temperature, pressure, or radon concentration at the point (n,m), the coefficients c, l, r, t, and b refer to the central, left, right, top, and bottom points, respectively, as viewed in the manner of Figure 1, and $s_{nm}$ is the inhomogeneous part of the equation. These equations, with appropriate boundary conditions, are solved using iterative techniques described by Patankar (1980), Loureiro (1987), and Loureiro, *et al.* (1990). The value of the field at iteration *i*, $\psi^{*i}_{nm}$, is given by

$$\psi^{*i}_{nm} = \psi^{*i-1}_{nm} + \omega\left[\psi^{i}_{nm} - \psi^{*i-1}_{nm}\right], \tag{16}$$

where $\psi^{i}_{nm}$ is the solutions of Equation 15 at iteration *i*, $\psi^{*i-1}_{nm}$ is the solution of Equation 16 at iteration *i*-1, and $\omega$ is the relaxation coefficient. Satisfactory results may generally be obtained for $\omega = 1.5$, except where temperature and pressure equations must be coupled, in which case $\omega$ must be at least 1 to ensure numerical stability. All results cited in this paper have been obtained with $\omega = 1$.

Boundary values are introduced into Equation 15 in a straightforward manner; all have fixed values, except for the pressure at a soil-gap interface, which requires special treatment. (The temperature and radon concentration at a soil-gap interface are treated conventionally. See Figure 2 and the discussions following Equations 1 and 12.) Let $p_{nm}$ be the pressure at an interface node. Initially, we set $\Delta P_b$ to the representative winter value of -5 Pa and $\Delta P_g$ to zero; $p_{nm}$ is found from the discrete form of Equation 4. After the first iteration, the pressure immediately outside the opening is known, and a relationship between this pressure, $p_{nm}$, and the average air speed at the opening can be found from the discrete form of Equation 5. A second expression involving $p_{nm}$ and the average speed is Equation 9. From the two equations, a new value of $p_{nm}$

is determined and used as a boundary value during the next iteration.

Iterations are permitted to continue until the residuals fall below a fixed tolerance; for results cited in this paper, the tolerance is $10^{-6}$. As a further check when a gap is present, the total rate of mass transport through the gap is compared to the transport rate across the soil surface. For results cited in this paper, the relative difference is always less than 0.1%.

The final step in the procedure is the calculation of the soil-gas and radon entry rates, using the discrete forms of equations 11 and 14.

## Model Predictions

In this section, we compare the predictions of two-dimensional cylindrical and three-dimensional rectangular versions of the model, give a brief description of the nature and magnitude of the soil-gas flows and radon concentrations predicted by the model, and discuss the relationship between the radon entry rate, the indoor radon concentration, and the soil permeability for the configuration depicted in Figures 1 and 2. For a more complete discussion of the influence of soil permeability on radon entry, see Revzan, 1990a. The influence of structural factors and construction practices on radon entry is the subject of Revzan and Fisk, 1990b.

For the comparison of the two models, we assume that the configuration is that of Figures 1 and 2 and that the soil is homogeneous. In the simulations, the permeability varied from $10^{-12}$ to $10^{-10}$ $m^2$. The basement cross-section for the three-dimensional model was square; in two sets of simulations, the length of a side was first taken equal to the cylinder diameter d and then equal to $d/\sqrt{2}$, the latter value giving a diagonal equal to d. The gap width was 0.003 m. The discrepancies in the predicted soil-gas flux (*i.e.*, entry rate per unit length of gap) were ~8% for all configurations, with the three-dimensional model making the lower prediction. The discrepancies in the radon concentration at the soil-gap interface were less than 1%, with the three-dimensional model predicting the higher value, so that the discrepancies in the predicted radon entry rate were on the order of 7%. Figure 3 shows the pressure immediately under the basement slab along the radius of the cylindrical cross-section and the half-diagonal of the square cross-section, both 5 m, for a basement pressure of -5 Pa. The slab-footer gap is 0.15 m from the wall, as shown in Figure 2. Generally, the three-dimensional model predicts a lower pressure gradient near the gap, and therefore a lower soil-gas entry rate than the cylindrical model. Since the perimeter of the square is less than that of the circle, the fluxes predicted by the two models are more nearly equal. Figure 3 does not illustrate the relatively high pressure gradient predicted by the three-dimensional model at the corners of the footer; however, the high gradients in these small regions do not significantly increase the total entry rate of soil gas or radon.

The nature of the soil gas flows predicted by the cylindrical model may be seen in Figures 4-6, which show streamlines for the configuration of Figures 1 and 2. The soil temperature, where used, is determined by the model assuming an outside air temperature of 0 °C, a basement temperature of 15 °C, and a soil temperature at 10 m depth of 10 °C, which is the assumed annual mean, so that conditions are typical of winter in a cold climate. Figure 4 illustrates the case of pure natural convection. Here $\Delta P_b = 0$, *i.e.*, the basement is at atmospheric pressure, so that the flow is a circulation toward the warmer basement wall. Figure 5 illustrates the case of pressure-

driven flow for isothermal soil for a basement pressure 5 Pa lower than atmospheric. All flow lines run from the surface to the 0.003 m wide slab-footer opening, which is the only gap in the basement shell. In Figure 6, the two cases are combined, so that both a circulation and a flow into the gap are present.

Normalized radon entry rates for the configuration of Figures 1 and 2 are plotted against the permeability of the homogeneous soil in Figure 7. The solid line shows the predicted entry rates for the complete model, with conduction and advection of heat included, *i.e.*, with the temperature and pressure equations coupled. The basement, outside, and deep soil temperatures are 15, 0, and 10 °C, respectively. The dashed line shows the predicted results for isothermal conditions. For the soil permeabilities of greatest practical interest ($10^{-10} - 10^{-12}$ m$^2$), the introduction of thermal effects increases the radon entry rate by 35-40%. The dotted line shows the predicted entry rates when heat advection is neglected but conduction is included. Advection of heat begins to become significant, for a basement pressure of -5 Pa, at a soil permeability of $10^{-10}$ m$^2$. Since the soil-gas speed is directly dependent on the product of $|\Delta P_b|$ and k, heat advection may be neglected when this product is less than ~$5 \times 10^{-10}$ Pa m$^2$.

The indoor radon concentration corresponding to a particular normalized entry rate depends on the radon concentration in the soil, the volume of the building, and the air-exchange rates between basement and outside, basement and living area, and living area and outside. A complete treatment of this subject is outside the scope of this paper, but in a simplified model in which the house is considered a single zone whose air is fully mixed, the indoor radon concentration, C, is given by

$$C = \frac{E_r C_\infty}{V \lambda}, \tag{17}$$

where V and $\lambda$ are, respectively, the volume and air-exchange rate of the house. For a house of volume 500 m$^3$ and air-exchange rate of 0.5 h$^{-1}$, whose surrounding soil has a (typical) $C_\infty$ of $3.5 \times 10^4$ Bq m$^{-3}$, $E_r$ (m$^3$ s$^{-1}$) must be multiplied by ~$5 \times 10^5$ to obtain the indoor radon concentration in Bq m$^{-3}$. For a homogeneous soil of permeability $10^{-11}$ m$^2$, the predicted indoor concentration is ~10 Bq m$^{-3}$. When a layer of high-permeability gravel is present under the basement slab, the predicted indoor concentration is a factor of 5 higher (Revzan and Fisk, 1990b).

The relation between the radon and soil-gas entry rates at any narrow opening may be approximated by

$$E_r = E_s C_{avg}, \tag{18}$$

where $C_{avg}$ is the average soil-gas radon concentration at the opening. By Darcy's law, $E_s$ is linearly dependent on soil permeability. Figure 7 shows, in contrast, that the relation between $E_r$ and k is not linear, particularly at high k. The departure from linearity is accounted for by the diminution in the radon concentration of the soil gas that enters the slab-footer gap as the soil permeability and soil-gas velocity increase. Figure 8 illustrates this point by showing the average normalized radon concentration at the slab-footer gap, plotted against the soil permeability, for the configuration of Figures 1 and 2.

## Model Verification

There are few data available to compare with the predictions of the model. However, a study of several houses in the Spokane River valley of Washington and Idaho (Turk, *et al.*, 1987) provides some information on permeabilities and entry rates for 14 houses, of which six had full concrete basements and one a basement and a small adjoining crawlspace. Since the results of permeability measurements are not precise, and since detailed information on the substructures and underlying soil are unavailable, we shall not discuss the houses individually, but rather compare the range of calculated entry rates with the predictions. The permeability of the soil underlying the entire area of the study appears to be on the order of $2 \times 10^{-10}$ m$^2$. The normalized radon entry rates are calculated from the data provided by Turk from the equation

$$E_r = \frac{CV\lambda}{C_\infty}, \tag{19}$$

where C is the time-averaged indoor radon concentration in the living area, measured in the winter, $\lambda$ is the time-averaged measured air-exchange rate, and $C_\infty$ is based on analysis of soil samples taken far from the houses. For the 7 houses which can be modeled reasonably well, the values of $E_r$ calculated from measured data range from $5.5 \times 10^{-4}$ to $3.2 \times 10^{-3}$ m$^3$ s$^{-1}$; the mean and standard deviation are $1.7 \times 10^{-3}$ and $1.1 \times 10^{-3}$ m$^3$ s$^{-1}$, respectively. For a soil permeability of $2 \times 10^{-10}$ m$^2$, no subslab gravel layer (no layer having been reported), and a slab-footer gap width of 0.003 m, the model predicts an entry rate of $3.8 \times 10^{-4}$ m$^3$ s$^{-1}$ when the basement-outside pressure difference is a nominal winter value of -5 Pa (Revzan, *et al.*, 1988; Revzan, 1989) and the basement, soil surface, and lower soil boundary temperatures are 15, 0, and 10 C, respectively.

The predicted entry rate is 22% of the calculated mean; the discrepancy may be accounted for by errors in the measurement of permeability. Some soils exhibit anisotropy in permeability (Nazaroff, 1988a), the permeability for air flow parallel to the soil surface being greater than that for flow perpendicular to the surface. It is unclear whether the measured permeability represents the permeability in one of the two directions or an average of the two. Furthermore, since the permeability measurements were made during the rainy season, it is possible that the average winter permeabilities exceed the measured value; permeability measured in water-saturated soil can easily be 0.3 of the dry value or even less (Nazaroff, 1988a). Perhaps more significantly, the errors in the measurements of soil permeability may be high. The assumption of a soil permeability of $1.4 \times 10^{-9}$ m$^2$, a factor of 7 greater than the measured value, leads to a predicted entry rate approximately equal to the mean of the values determined from the data.

On the other hand, the discrepancy will be larger if the average $|\Delta P_b|$ is smaller than 5 Pa, if the basement-outside temperature difference is smaller than 15 °C, if the gap width is less than 0.003 m, if the soil block from which each house may draw radon is smaller than we have estimated or if the entry rates have been underestimated. The entry rates were calculated from radon concentrations measured in the living areas on the assumption that forced-air furnaces (present in 5 of the 7 houses) assured good mixing of air in most of the houses. If basement radon levels were significantly higher than those upstairs, then the entry rates calculated from equation 19, with C equal to the basement concentration, would be higher than the stated values.

The highest and lowest entry rates determined from measurements differ by a factor of 6. Since the regression of the entry rate on the permeability has an $R^2$ of 0.01, the disparity cannot be accounted for by differences in soil permeabilities, and we must infer that there are differences in structures, sites, and soils which have not been taken into account. A peripheral opening in the basement shell is a normal consequence of building practices. Additional openings may exist as the result of penetrations for utilities or of cracking of the concrete. However, an examination of the predictions of the model shows that the addition of openings serves primarily to redistribute the flow of soil gas while increasing the overall entry rate by a factor of 1.5 at most (Revzan and Fisk, 1990b). Radon may also enter through permeable block walls (Garbesi and Sextro, 1989).

Although it is not usual for gravel to be placed under a slab when the soil itself is well drained (*i.e.*, highly permeable), it may be that a gap between slab and soil or disturbance of the soil during construction creates a high-permeability region under the slab. The assumption of a soil permeability of $2 \times 10^{-10}$ m$^2$ everywhere except for a region of permeability $10^{-9}$ and thickness 0.15 m under the slab leads to a predicted entry rate of $9.0 \times 10^{-4}$ m$^3$ s$^{-1}$, which is 53% of the mean of the entry rates calculated from the data. The entry rate remains high ($5.8 \times 10^{-4}$ m$^3$ s$^{-1}$) even when the thickness is as low as 0.01 m. As the permeability of the 0.01 m layer approaches infinity, so that there is a gap between the concrete slab and the soil (not to be confused with the slab-footer gap), the entry rate approaches $1.3 \times 10^{-3}$ m$^3$ s$^{-1}$, which is 76% of the mean. If the thickness is reduced to that of the slab-footer gap itself, *i.e.*, 0.003 m, the entry rate is $1.2 \times 10^{-3}$ m$^3$ s$^{-1}$.

In sum, the radon entry rate through a slab-footer gap predicted by the model, assuming a homogeneous and isotropic soil, is considerably lower than the total entry rate inferred from measured data. The discrepancy may be accounted for by failure to take into account permeability anisotropy, underestimation of the permeability of the regions immediately adjacent to openings in the building shell, and by the possible presence of permeable walls and additional openings in the building shell.

## Summary and Conclusions

We have modified the three-dimensional steady-state model of Loureiro, *et al.* (1990) to simulate pressure and radon concentration fields in the vicinity of a cylindrically-symmetrical representation of a basement. The boundaries of the simulation space are the outside of the basement wall, slab, and footer, the mouth of the slab-footer gap, and the outer limits of the soil block associated with the basement. The basement may be warmer than the soil and the outside; natural convection (buoyancy) of soil gas resulting from this condition is included in the model, and has been shown to increase radon entry by approximately 40%. Three important subjects have not been examined. First, the effects of temporal variations in barometric pressure, which may be far greater in amplitude than the steady-state basement- outside pressure differences, have been neglected. A time-dependent model is being developed to determine if these effects, which may be significant when the soil permeability is low, are an important factor in radon entry. Second, we have neglected soil moisture, which affects both soil permeability and soil-gas radon concentration. Moisture is certainly an important factor in the production and transport of radon in soil, and the extension of the model to deal with its influence, even in an unsophisticated manner, is

clearly necessary. Third, permeability anisotropy has been neglected. The model is being modified to permit the permeability to be treated as a tensor, rather than as a scalar.

In a comparison of radon entry rates predicted by the model with those determined from a study of the Spokane, WA region, we have chosen values of the basement pressure and temperature that are typical of winter in cold regions and soil permeabilities that are close to those measured. If the soil is assumed to be homogeneous and isotropic, with permeability equal to the mean of the measured values, the predicted radon entry rate is 22% of the mean of the observations. The observed radon entry rates may then be accounted for by assuming that a narrow gap exists between the basement slab and the soil, by assuming that there are gaps in the basement shell in addition to the slab-footer gap, and by taking the soil permeability to be somewhat higher than the measured value, which is highly uncertain. Further verification of the model requires a more completely characterized site and the maintenance of steady-state conditions; work on an experimental structure that meets these conditions is now proceeding (Fisk, *et al.*, 1989).

**Acknowledgements**

We should like to thank our colleagues K. Garbesi, R. Sextro, and Y. Tsang for their critical examination of this paper.

This work was supported by the Director, Office of Energy Research, Office of Health and Environmental Research, Ecological Research Division, Human Health and Assessments Division, and Pollutant Characterization and Safety Research Division and by the Assistant Secretary for Conservation and Renewable Energy, Office of Building and Community Systems, Building Systems Division of the U.S. Department of Energy (DOE) under Contract No. DE-AC03-76SF00098.

## References


Baker, P.H., Sharples, S., Ward, I.C. (1989) "Air Flow Through Cracks" Building and Environment, 22(4), 293-304.

Bejan, A. (1984) Convection Heat Transfer, New York, Wiley.

Dimbylow, P.J. (1987). "The Solution of the Pressure Driven Flow Equation for Radon Ingress through Cracks in Concrete Foundations" Radiation Protection Dosimetry, 18(3), 163-167.

Ene, H.I. and Polisevski, D. (1987) Thermal Flow in Porous Media, Dordrecht, Reidel.

Feustel, H.E. and Sherman, M.H. (1989) "A Simplified Model for Predicting Air Flow in Multizone Structures" Energy and Buildings, 13, 217-230.

Fisk, W.J., Flexser, S., Gadgil, A.J., Holman, H.-Y., Modera, M.P., Narasimhan, T.N., Nuzum, T., Revzan, K.L., Sextro, R.G., Smith, A.R., Tsang, Y.W., and Wollenberg, H.A. (1989) Monitoring and Modeling for Radon Entry into Basements: A Status Report for the Small Structures Project, Lawrence Berkeley Laboratory Report LBL-27962.

Garbesi, K., Sextro, R.G. (1990) "Modeling and Field Evidence of Pressure-Driven Entry of Soil Gas into a House through Permeable Below-Grade Walls" Environmental Science and Technology, 23, 1481-1487.

Loureiro, C.O. (1987) Simulation of the Steady-State Transport of Radon from Soil into Houses with Basements under Constant Negative Pressure, Lawrence Berkeley Laboratory Report LBL-24378.

Loureiro, C.O., Abriola, L.M., Martin, J.E., and Sextro, R.G. (1990) "Three Dimensional Simulation of Radon Transport into Houses Under Constant Negative Pressure" Environmental Science and Technology, 24, 1338-1348.

Mowris, R.J. and Fisk, W.J. (1987) "Modeling the Effects of Exhaust Ventilation on Radon Entry Rates and Indoor Radon Concentrations" Health Physics, 54, 491-501.

Nazaroff, W.W. (1988a) "Soil as a Source of Indoor Radon: Generation, Migration, and Entry" In Nazaroff, W.W. and Nero, A.V., eds., Radon and its Decay Products in Indoor Air, New York, Wiley, pp 57-112.

Nazaroff, W.W. (1988b) "Predicting the Rate of $^{222}Rn$ Entry from Soil into the Basement of a Dwelling due to Pressure-Driven Air Flow" Radiation Protection Dosimetry, 24(1), 199-202.

Nazaroff, W.W. and Sextro, R.G. (1989) "Technique for Measuring the Indoor $^{222}Rn$ Source Potential of Soil" Environmental Science and Technology, 23, 451-458.

Nero, A.V., Schwehr, M.B., Nazaroff, W.W., and Revzan, K.L. (1986) "Distribution of Airborne Radon-222 Concentrations in U.S. Homes" Science, 234, 992-997.

Nero, A.V. (1988a) "Radon and Its Decay Products in Indoor Air: An Overview" In Nazaroff, W.W. and Nero, A.V., eds., Radon and its Decay Products in Indoor Air, New York, Wiley, pp 1-53.

Nero, A.V., Revzan, K.L., and Sextro, R.G. (1988b) Appraisal of the U.S. Data on Indoor Radon Concentrations, Lawrence Berkeley Laboratory Report LBL-24345.

Oke, T.R. (1987) Boundary Layer Climates, New York, Methuen.

Patankar, S.V. (1980) Numerical Heat Transfer and Fluid Flow, New York, Hemisphere.

Revzan, K.L., Turk, B.H., Harrison, J., Nero, A.V., and Sextro, R.G. (1988) "Parametric Modelling of Temporal Variations in Radon Concentrations in Homes" IEEE Transactions in Nuclear Science, 35(1), 550-555.

Revzan, K.L. (1989) Radon Entry, Distribution, and Removal in Two New Jersey Houses with Basements, Lawrence Berkeley Laboratory Report LBL-26830.

Revzan, K.L. (1990a) Modeling Radon Entry into Houses with Basements: The Influence of Soil Characteristics, Lawrence Berkeley Laboratory Report LBL-28109.

Revzan, K.L. and Fisk, W.J. (1990b) Modeling Radon Entry into Houses with Basements: The Influence of Structural Factors, Lawrence Berkeley Laboratory Report LBL-28267. Submitted to Environmental Science and Technology.

Sherman, M.H., Grimsrud, D.T., and Diamond, R.C. (1979) Infiltration-Pressurization Correlation: Surface Pressures and Terrain Effects, Lawrence Berkeley Laboratory Report LBL-8785.

Turk, B.H., Prill, R.J., Grimsrud, D.T., Moed, B.A., and Sextro, R.G. (1987) Radon and Remedial Action in Spokane Valley Homes, Volume 1: Experimental Design and Data Analysis, Lawrence Berkeley Laboratory Report LBL-23430.

Zapalac, G.H. (1983) "A Time-Dependent Method for Characterizing the Diffusion of Radon-222 in Concrete" Health Physics, 45(2), 377-283.

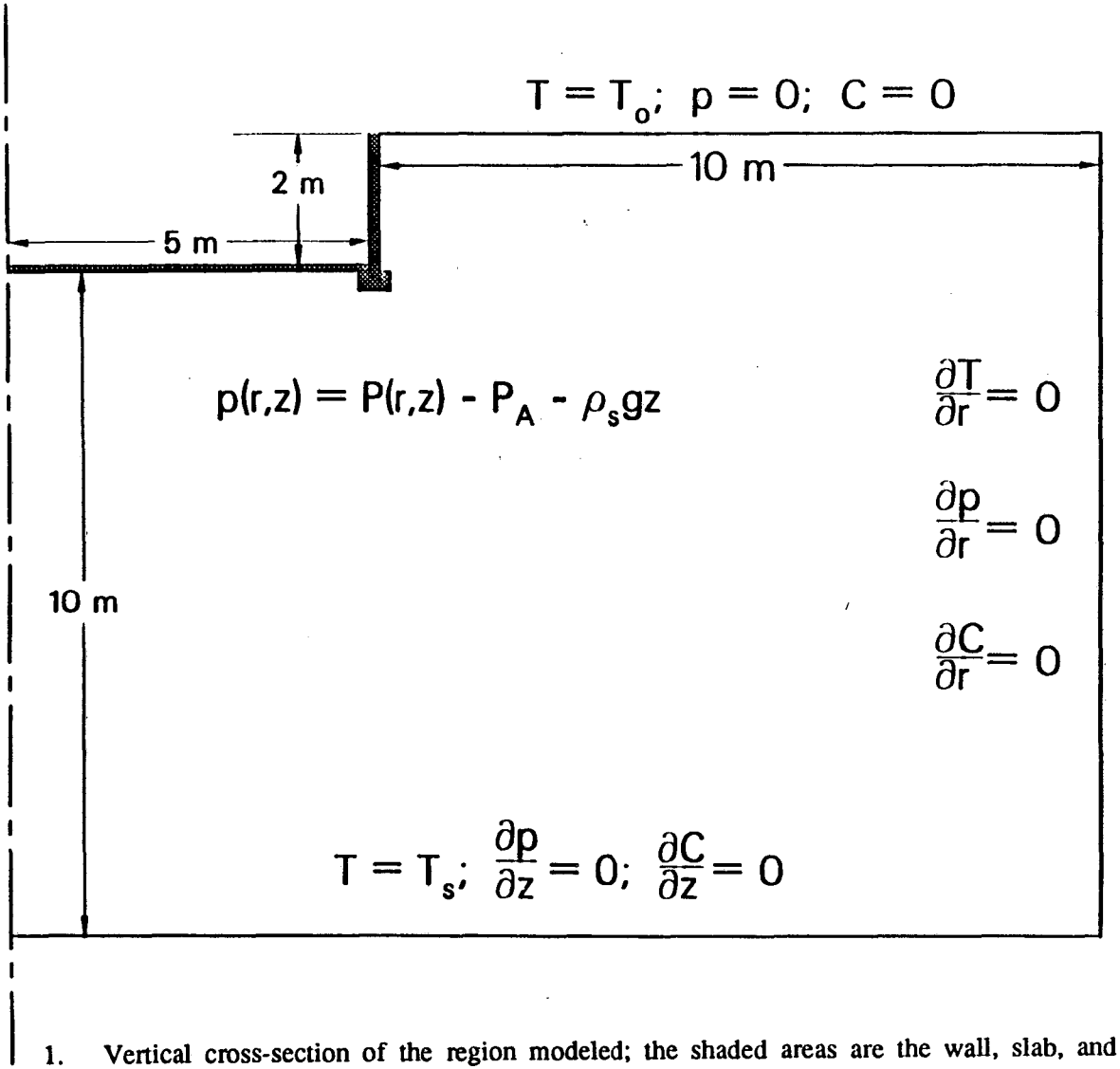


1. Vertical cross-section of the region modeled; the shaded areas are the wall, slab, and footer. The boundary conditions for the temperature (T), pressure (p), and radon concentration (C) fields at the soil surface and at the outer and lower soil boundaries are shown in the appropriate locations. The definition of the pressure p is also shown; P is the absolute pressure, $P_A$ is the atmospheric pressure, $\rho$ is the air density and $\rho_s$ is its value at the lower soil boundary, g is the acceleration of gravity, and z is the vertical coordinate, taken positive downward.

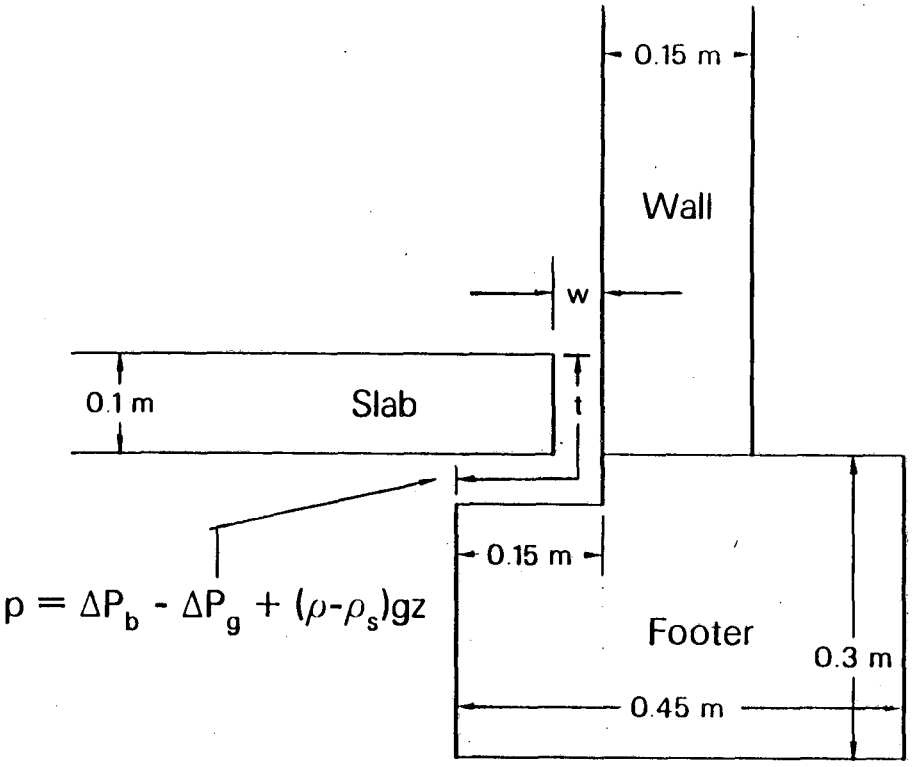


Vertical surfaces: $T = T_b$; $\frac{\partial p}{\partial r} = 0$; $\frac{\partial C}{\partial r} = 0$

Horizontal surfaces: $T = T_b$; $\frac{\partial p}{\partial z} = (\rho-\rho_s)g$; $\frac{\partial C}{\partial z} = 0$

2. Detail of the vertical cross-section of the region modeled. The width of the slab-footer and slab-wall gaps is shown greatly exaggerated. The boundary conditions at the vertical and horizontal concrete surfaces are given below the figure. For the temperature and concentration fields, the vertical boundary conditions also apply at the soil-gap interface; the boundary condition for the pressure at the interface is shown just below the basement slab. $T_b$ is the basement temperature, $\Delta P_b$ is the pressure difference between the basement and the outside, $\Delta P_g$ is the pressure difference between the basement and the soil-gap interface, $\rho$ is the soil-gas (air) density generally, $\rho_s$ is the soil-gas density at the lower soil boundary, w is the gap width and t the gap thickness. The definition of the pressure p is given in the text and in Figure 1.

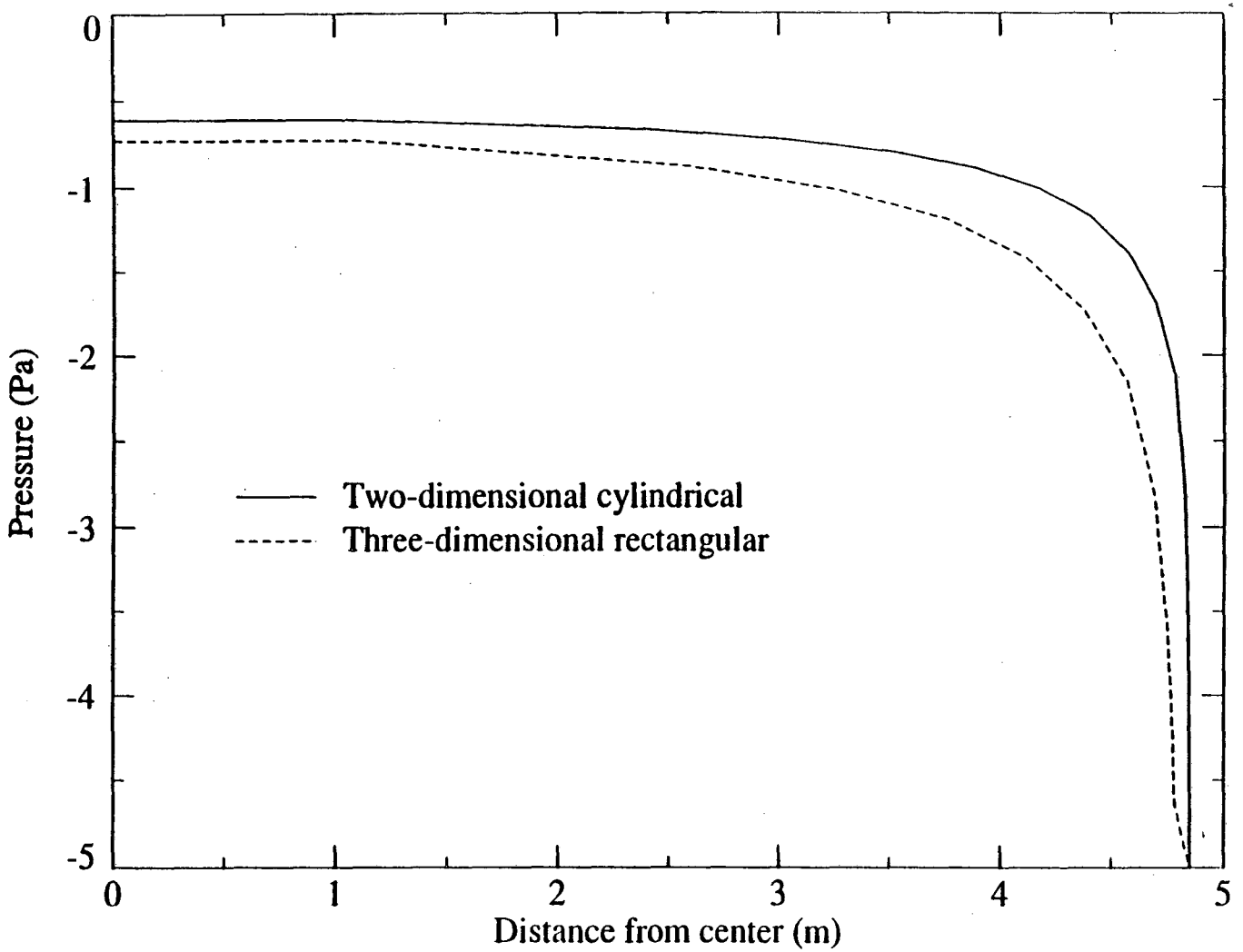


3. Pressure immediately under the basement slab for the two-dimensional cylindrical and three-dimensional rectangular models. The configuration is that of Figures 1 and 2. The soil is homogeneous. The three-dimensional model has a square horizontal cross-section whose diagonal is equal to the diameter of the cylindrical horizontal cross-section of the two-dimensional model (10 m). The basement pressure is -5 Pa with respect to the atmosphere. The pressure drop across the slab-footer-wall gap is negligible, so that the pressure at the soil-gap interface, which is 4.85 m from the center, is ~ -5 Pa as well.

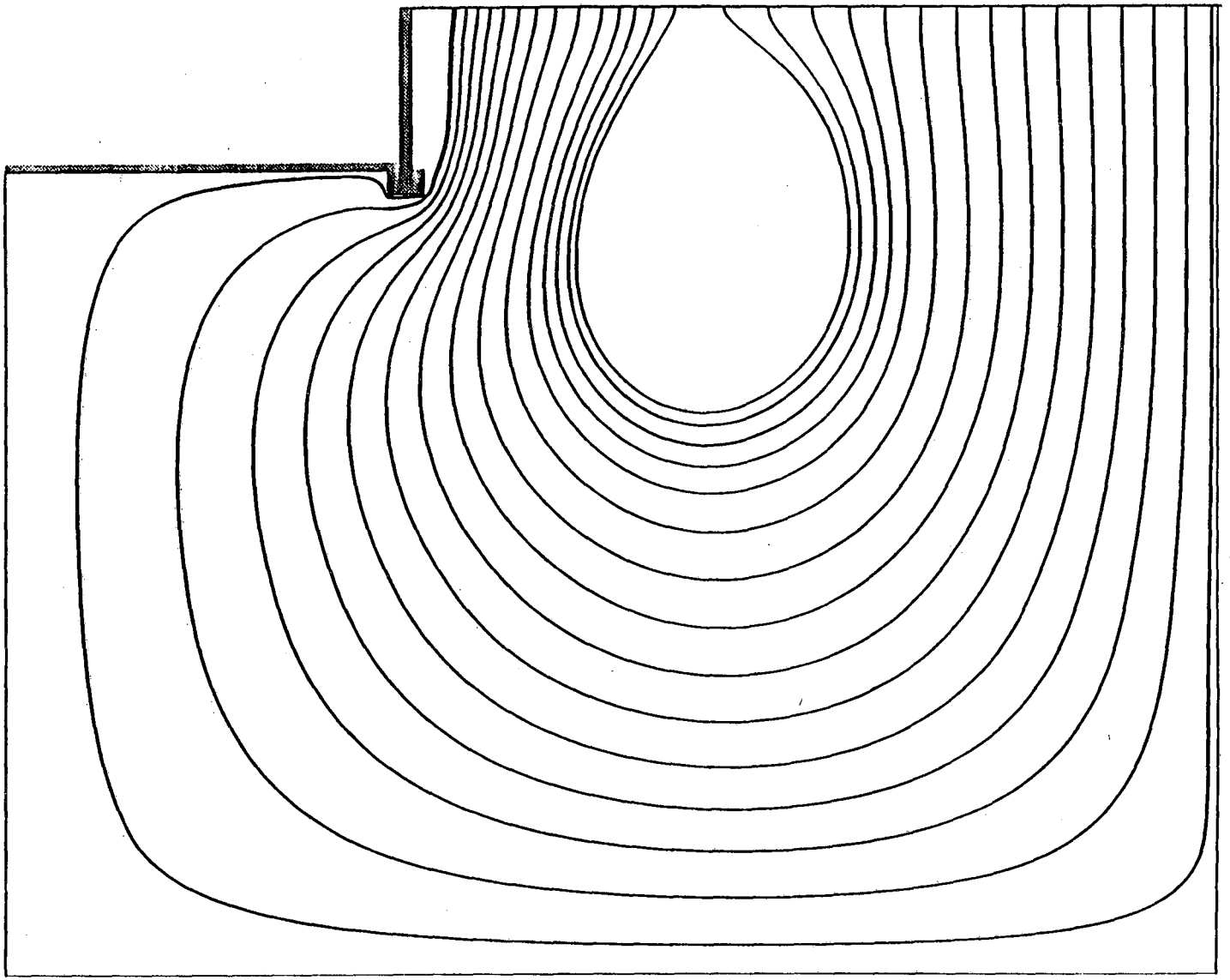

4. Vertical cross-section of a basement and the surrounding soil, with streamlines; the direction of flow is clockwise. In this case there is no pressure difference between basement and outside, so that the flow is a circulation due to natural convection. The temperatures of the basement, the soil surface, and the lower soil boundary are 15, 0, and 10 °C, respectively.

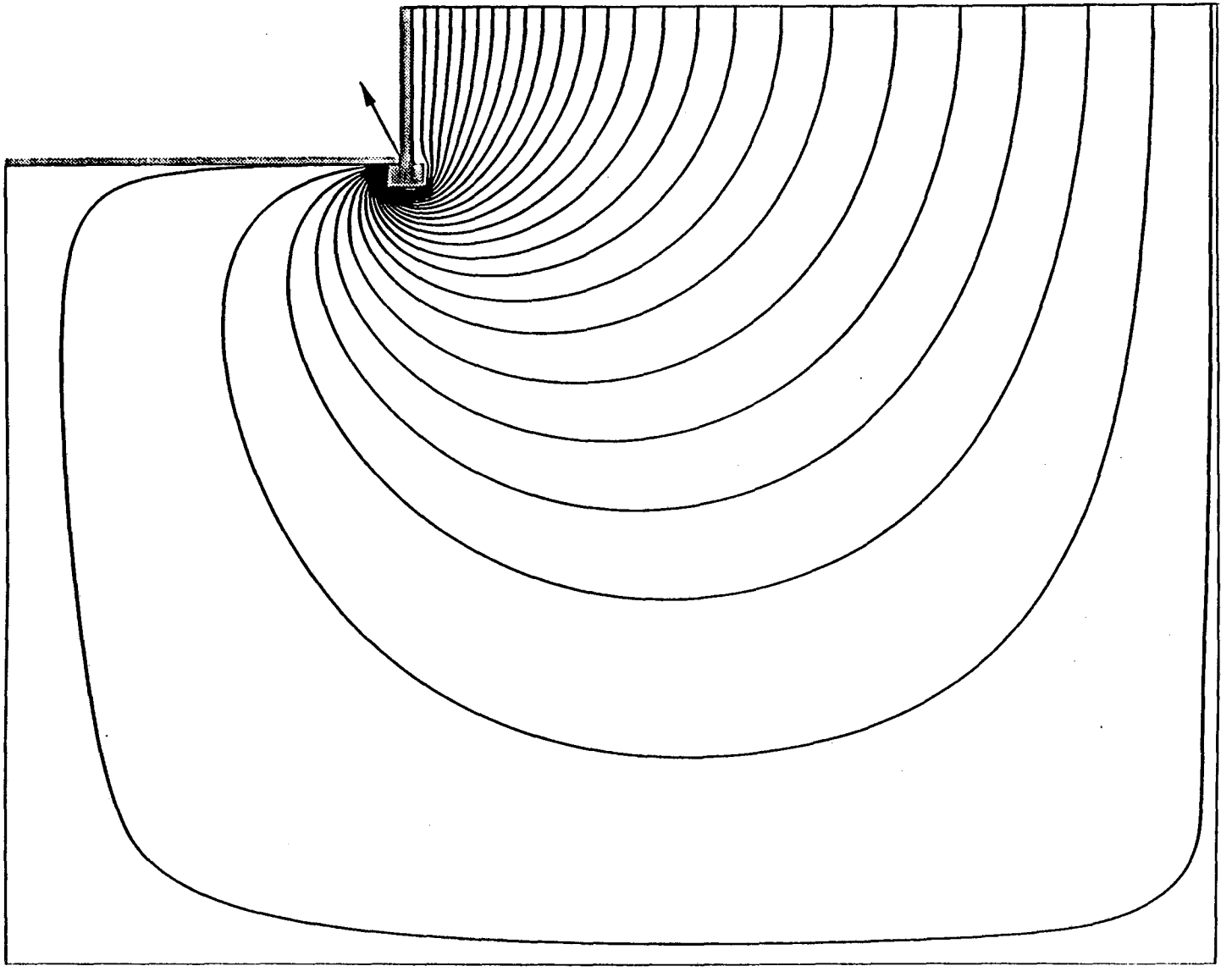

5. Vertical cross-section of a basement and the surrounding soil, with streamlines; the direction of flow is clockwise. In this case the flow is due entirely to forced convection; the basement pressure is 5 Pa below that of the atmosphere.

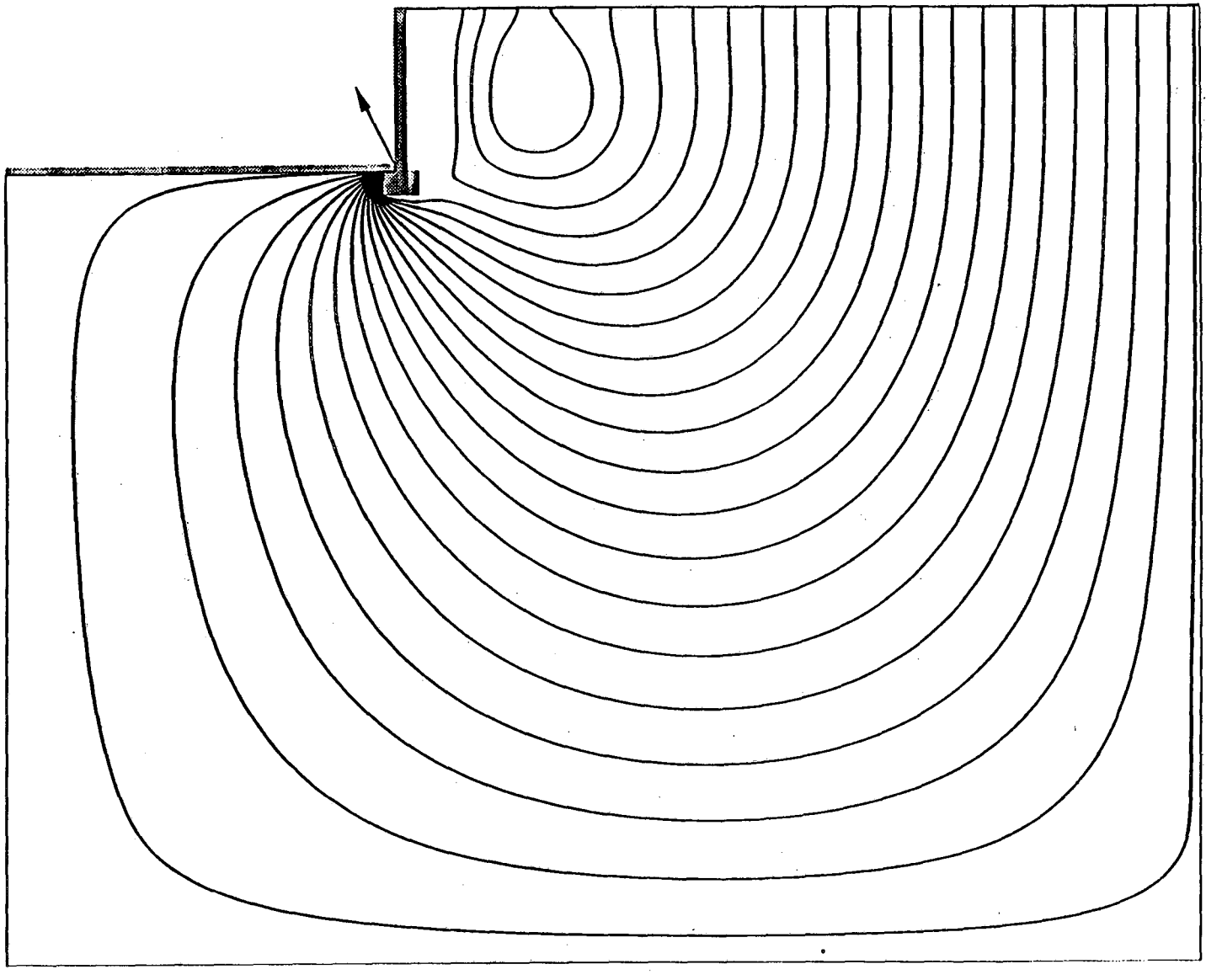

6. Vertical cross-section of a basement and the surrounding soil, with streamlines; the direction of flow is clockwise. In this case both forced and natural convection are present. The basement pressure is 5 Pa below that of the atmosphere. The temperatures of the basement, the soil surface, and the lower soil boundary are 15, 0, and 10 C, respectively.

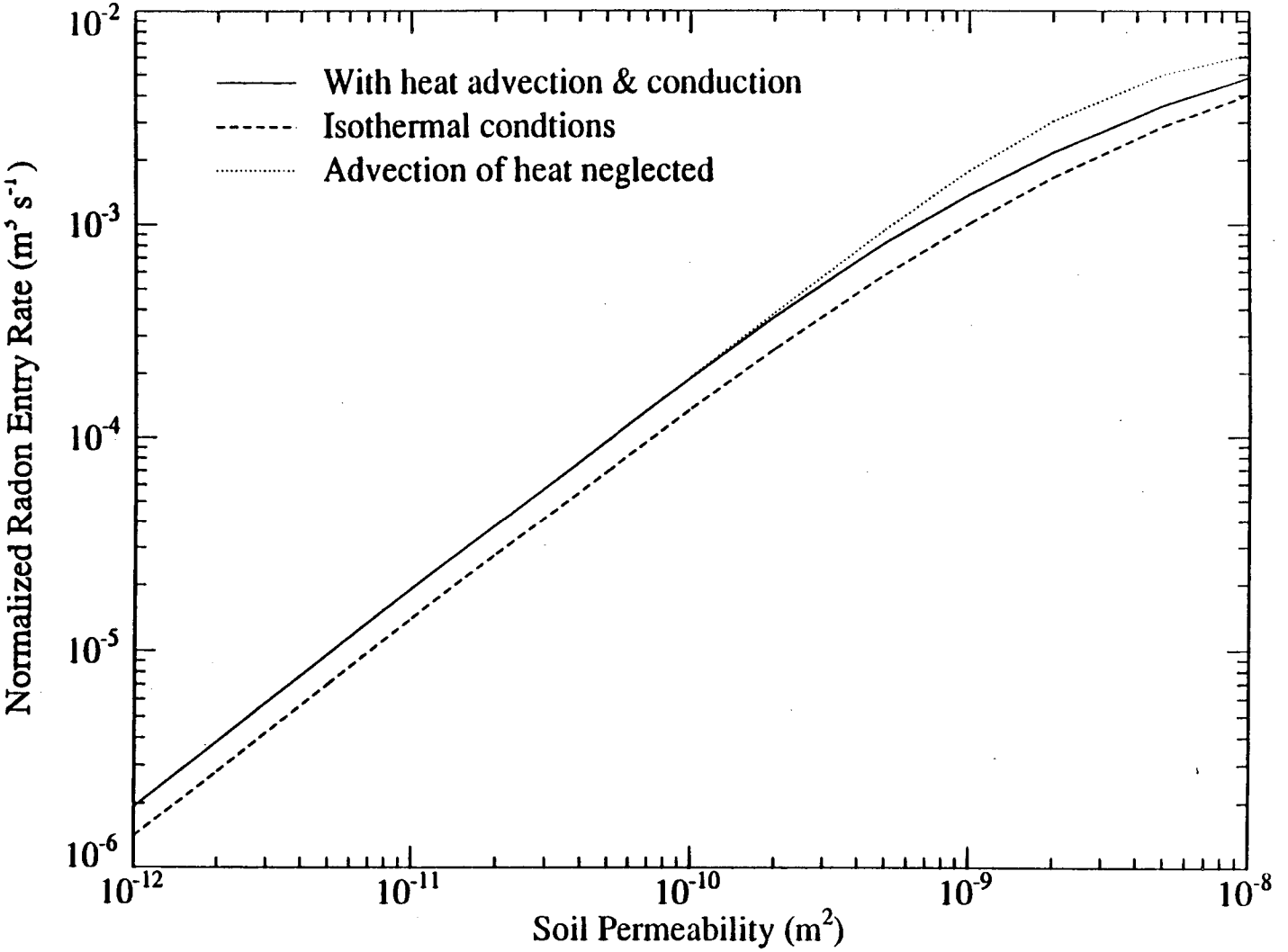


7. The predicted normalized radon entry rate into the slab-footer gap of a basement, plotted against soil permeability, for the configuration of Figures 1 and 2. The basement is 5 Pa below atmospheric pressure. The solid line shows the predicted rates when both thermal conduction and convection are included in the model. The basement, outside, and deep soil temperatures are 15, 0, and 10 °C, respectively. The dashed line shows the predictions for isothermal conditions. The dotted line shows the predictions when thermal convection is neglected.

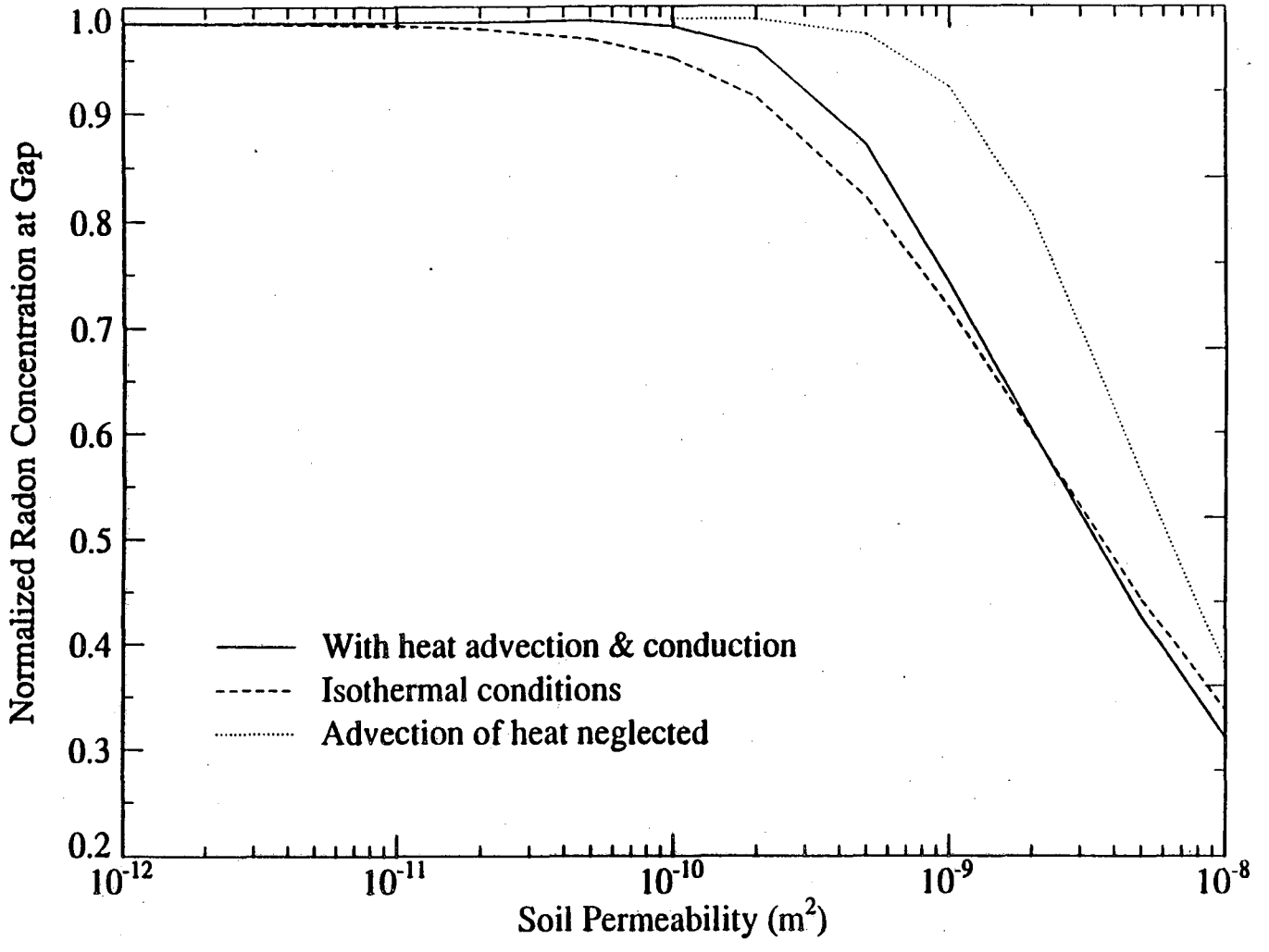


8. The predicted average normalized radon concentration in the slab-footer gap of a basement, plotted against soil permeability, for the configuration of Figures 1 and 2. The basement 5 Pa below atmospheric pressure. The solid line shows the predicted concentrations when both thermal conduction and convection are included in the model. The basement, outside, and deep soil temperatures are 15, 0, and 10 °C, respectively. The dashed line shows the predictions for isothermal conditions. The dotted line shows the predictions when thermal convection is neglected.

LAWRENCE BERKELEY LABORATORY
UNIVERSITY OF CALIFORNIA
INFORMATION RESOURCES DEPARTMENT
BERKELEY, CALIFORNIA 94720